Electronic Supplementary Material (ESI) for Chemical Communications

A new Al-MOF based on an unique column-shaped inorganic building unit exhibiting strongly hydrophilic sorption behaviour

Helge Reinsch[a], Bartosz Marszałek[b], Julia Wack[c], Jürgen Senker[c], Barbara Gil[b], Norbert Stock[a]

[a] *Institute of Inorganic Chemistry, Christian-Albrechts-Universität Kiel, Max-Eyth-Straße 2, 24118 Kiel, Germany; E-mail: stock@ac.uni-kiel.de*

[b] *Faculty of Chemistry, Jagiellonian University, ul. Ingardena 3, 30-060 Kraków, Poland*

[c] *Inorganic Chemistry I, Universiät Bayreuth, Universitätsstaße. 30, 95447 Bayreuth, Germany*

Supplementary Information

S1: Materials and Methods

Chemicals. $AlCl_3 \cdot 6H_2O$ (Riedel-de Haen, ≥99%), terephthalic acid (H_2BDC) ABCR, 98 %), 2-aminoterephthalic acid ($H_2BDC\text{-}NH_2$, Fluka, ≥98%), 2-propanol (BASF, purum) were used as purchased. The synthesis was performed in custom made Teflon inserts in steel autoclaves with a volume of 30 mL. X-ray powder diffraction data for the cell refinement was collected on a Panalytical Xpert Highscore diffractometer in reflection geometry. Temperature dependent X-ray powder diffraction data was measured on a STOE Stadi-P diffractometer in transmission geometry equipped with an image plate detector (IPDS) using Cu-$K_{\alpha 1}$ radiation. The XRPD-synchrotron data was collected at beamline G3 at the DORIS-accelerator ring at DESY, Hamburg with a wavelength of 1.54295 Å in transmission geometry. Therefore, the sample was transferred into a 0.5 mm capillary. One dimensional solid state Magic-Angle-Spinning Nuclear Magnetic Resonance spectra were acquired on the APOLLO console (Tecmag) at the magnetic field of 7.05 T (Magnex). The one dimensional ^{27}Al MAS NMR spectra was recorded using the 2 μs rf pulse (π/6 flipping angle), 8 kHz spinning speed, and 1000 scans with acquisition delay 1 s.

The ^{27}Al MQMAS spectrum was measured with a Bruker Avance II 300 spectrometer operating at 7.05 T with a resonance frequency for ^{27}Al of 78.2045 MHz. The sample was packed in a ZrO_2 rotor with an outer diameter of 2.5 mm and mounted in a standard triple resonance MAS probe. The experiment was carried out at a rotation frequency of 25 kHz, using a three-pulse sequence[1] with nutation frequencies of 110 kHz for the excitation (2.2 μs) and conversion (1.2 μs) and 16 kHz for the selective 90° pulse. The coherence pathway (0→±3→-1) was selected via a cog-wheel phase cycle COG60{11,1,0;30}.[2] During t_1 and t_2 a cw(continuous wave)-decoupling with a nutation frequency of 45 kHz was applied, while the recycle delay was set to 1s.

Two dimensional FTIR spectra were recorded with a Bruker Tensor 27 spectrometer equipped with an MCT detector and working with the spectral resolution of 2 cm^{-1}. For the IR experiment a silicon wafer was covered by a thin layer of the material by evaporating on its surface a few drops of the CAU-6 dispersion in methanol.

The thermogravimetric analysis was carried out using a NETSCH STA 409 CD analyzer. The samples were heated in Al_2O_3 crucibles at a rate of 4 K min^{-1} under a flow of air (75 ml/min). The TG data were corrected for buoyancy and current effects. Sorption experiments were performed using a Belsorp-max instrument (BEL JAPAN INC.). The molecular modelling software used was Materials Studio 5.0.

S2: High-Throughput Investigations

CAU-6 and Al-MIL-68 were initially obtained from one single HT-experiment. The synthesis was carried out in a Teflon-lined HT-reactor using microwave-assisted heating (AntonPaarAnton Paar Synthos 3000 multimode microwave unit employing a 4x24MG5 rotor). The reaction temperature was set to 120 °C and the reaction time was 4 h. The composition of the reaction mixtures is given in Tab. S1. The observed tendencies and products are represented in Fig. S1.

Tab. S1: Composition of the reaction mixtures in the initial HT-experiment.

Reactor No	linker	n (linker) [mmol]	n ($AlCl_3 \cdot 6H_2O$) [mmol]	m (linker) [mg]	m ($AlCl_3 \cdot 6H_2O$) [mg]	V 2-propanol [µL]
1	$H_2BDC\text{-}NH_2$	0.066	0.033	12	8	1000
2	$H_2BDC\text{-}NH_2$	0.066	0.066	12	16	1000
3	$H_2BDC\text{-}NH_2$	0.066	0.099	12	24	1000
4	$H_2BDC\text{-}NH_2$	0.066	0.132	12	32	1000
5	$H_2BDC\text{-}NH_2$	0.066	0.199	12	48	1000
6	$H_2BDC\text{-}NH_2$	0.066	0.265	12	64	1000
7	$H_2BDC\text{-}NH_2$	0.132	0.066	24	16	1000
8	$H_2BDC\text{-}NH_2$	0.132	0.132	24	32	1000
9	$H_2BDC\text{-}NH_2$	0.132	0.199	24	48	1000
10	$H_2BDC\text{-}NH_2$	0.132	0.265	24	64	1000
11	$H_2BDC\text{-}NH_2$	0.132	0.397	24	96	1000
12	$H_2BDC\text{-}NH_2$	0.132	0.530	24	128	1000
13	H_2BDC	0.055	0.055	9	13	1000
14	H_2BDC	0.055	0.110	9	27	1000
15	H_2BDC	0.055	0.221	9	53	1000
16	H_2BDC	0.055	0.442	9	107	1000
17	H_2BDC	0.110	0.110	18	27	1000
18	H_2BDC	0.110	0.221	18	53	1000
19	H_2BDC	0.110	0.442	18	107	1000
20	H_2BDC	0.110	0.662	18	160	1000
21	H_2BDC	0.221	0.221	37	53	1000
22	H_2BDC	0.221	0.442	37	107	1000
23	H_2BDC	0.221	0.883	37	213	1000
24	H_2BDC	0.221	1.104	37	266	1000

Thus $H_2BDC\text{-}NH_2$ was employed in two different absolute concentrations in six different molar ratios $H_2BDC\text{-}NH_2$: $AlCl_3{\cdot}6H_2O$. H_2BDC was employed in three different absolute concentrations in four different molar ratios H_2BDC : $AlCl_3{\cdot}6H_2O$.

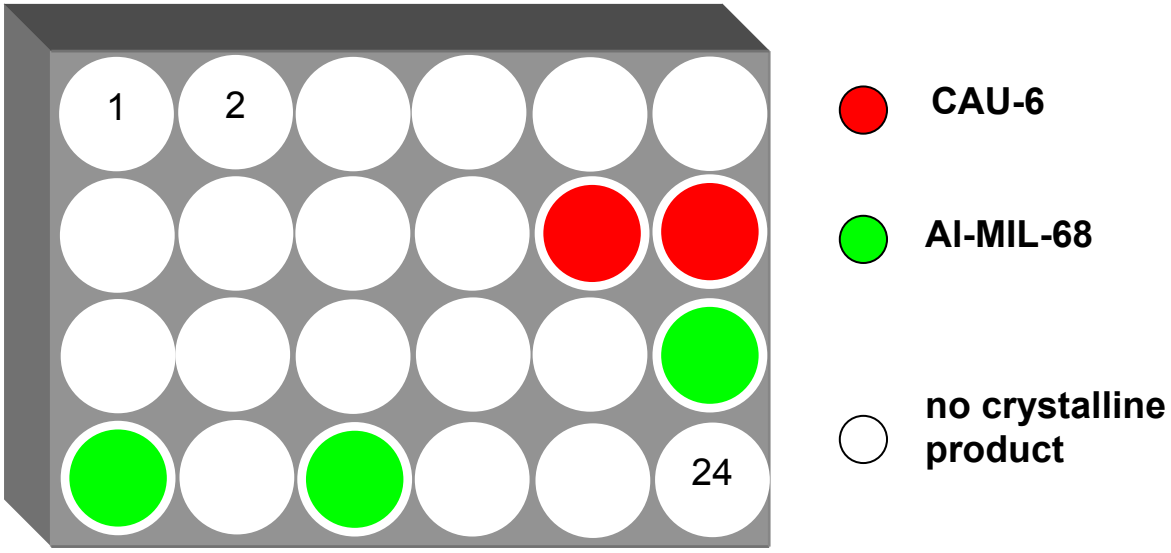

Fig. S1: Products that were obtained form the initial HT-experiment.

Only in few vessels, the formation of a crystalline product was observed. CAU-6 is only formed at high concentrations of $H_2\text{-}BDC\text{-}NH_2$ and if $AlCl_3{\cdot}6H_2O$ is used in large excess (molar ratio $H_2BDC\text{-}NH_2$: $AlCl_3{\cdot}6H_2O$ < 1 : 3). Al-MIL-68 is obtained from reaction mixtures with medium and high concentrations of H_2BDC and if at least equal amounts of $AlCl_3{\cdot}6H_2O$ are used (molar ratio H_2BDC : $AlCl_3{\cdot}6H_2O$ < 1 : 1). Subsequent optimization and upscaling of the reaction conditions led to the synthesis procedures given in S3 and S4.

S3: Data for Al-MIL-68

For the up-scaled synthesis 300 mg (1.8 mmol) terephthalic acid, 2.2 g $AlCl_3 \cdot 6H_2O$ (9.1 mmol) and 10 mL 2-propanol were heated in a Teflon-lined autoclave in 4 h to 130°C, held at this temperature for 12 h and cooled down to room temperature during 4 h. The product exhibits the MIL-68-topology, as shown by XRPD-measurements (Fig. S2).

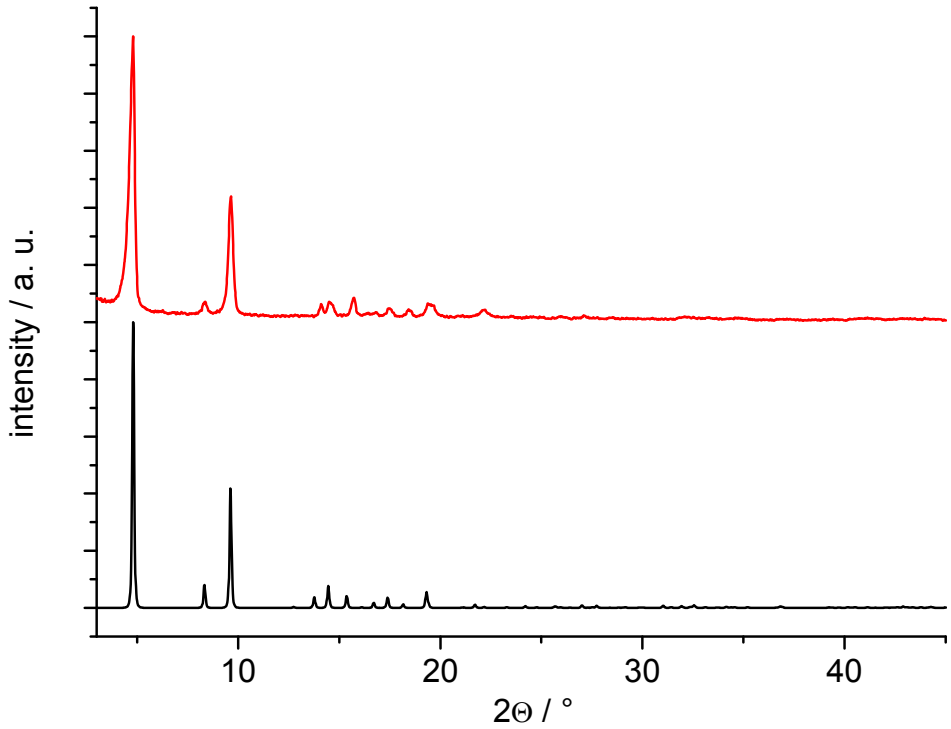

Fig. S2: Powder pattern of the obtained Al-MIL-68 (red line), in comparison with simulated data (black line).[3]

S4: Details of Synthesis and Characterisation of CAU-6

Optimized synthesis. 150 mg (0.83 mmol) $H_2BDC\text{-}NH_2$, 800 mg (3.32 mmol) $AlCl_3{\cdot}6H_2O$ and 5 mL 2-propanol were transferred into a Teflon-lined autoclave and mixed thoroughly. It should be mentioned that the synthesis yields the title compound only if Teflon-lined reactors are used, while the reaction in glass vessels result in X-ray amorphous products. The mixture was heated slowly during twelve hours to 120 °C, held at this temperature for twelve hours and cooled to room temperature over twelve hours. The filtered product was treated in 300 mL water by stirring for twelve hours, filtered again and dried under ambient conditions. This washing procedure was repeated four more times, and the final product was obtained as yellow, microcrystalline powder (Fig. S5). During the washing process, the molar ratio of Al:Cl was decreased from 1:1 to 13:6, as measured by EDX-analysis. Furthermore, the cell parameters are slightly shifted (Fig S3, S4). Elemental analysis of the final product: C 25.2 %, H 4.9 %, N 3.2 %. Theoretical values based on the sum formula $[Al_{13}(OH)_{27}(H_2O)_6(BDC\text{-}NH_2)_3Cl_6(C_3H_7OH)_6]$: 24.9 %, H 5.0 %, N 2.1 %.

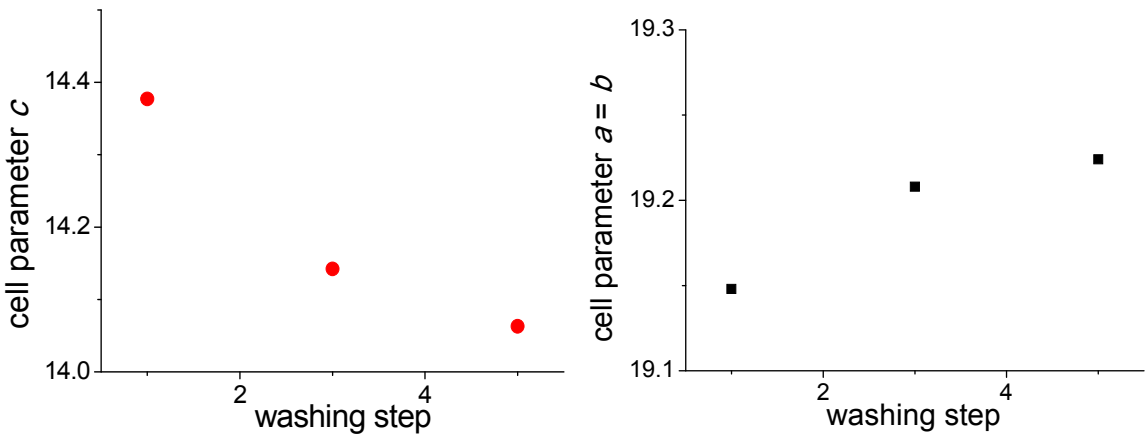

Fig. S3: Cell parameters for *c* (left) and *a* = *b* (right), as obtained by the le Bail-Fit method. Error bars lie within the symbols.

.

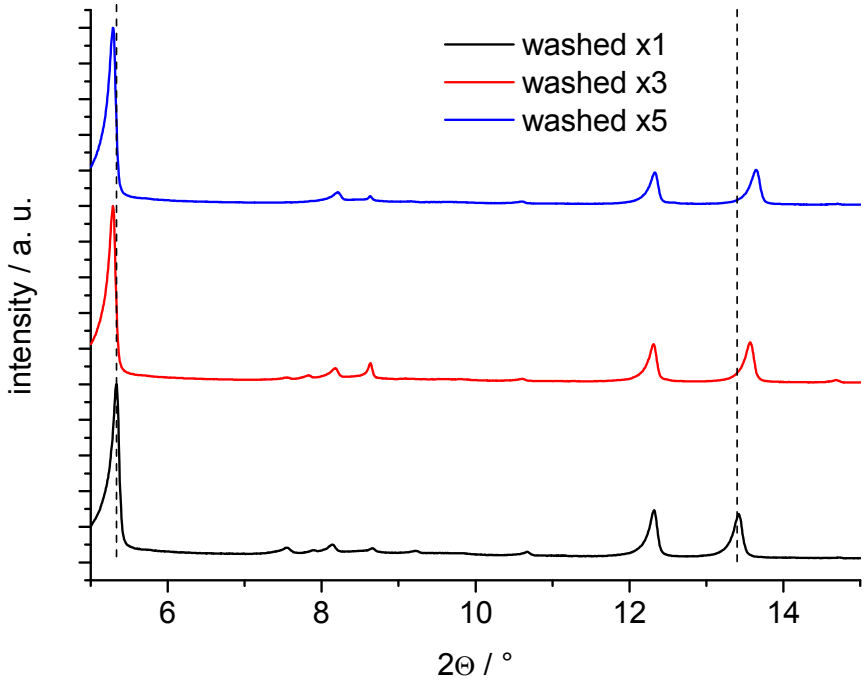

Fig. S4: Low-angle region of the powder patterns measured after washing 1, 3 and 5 times. The dashed lines were inserted to guide the eye.

SEM micrographs

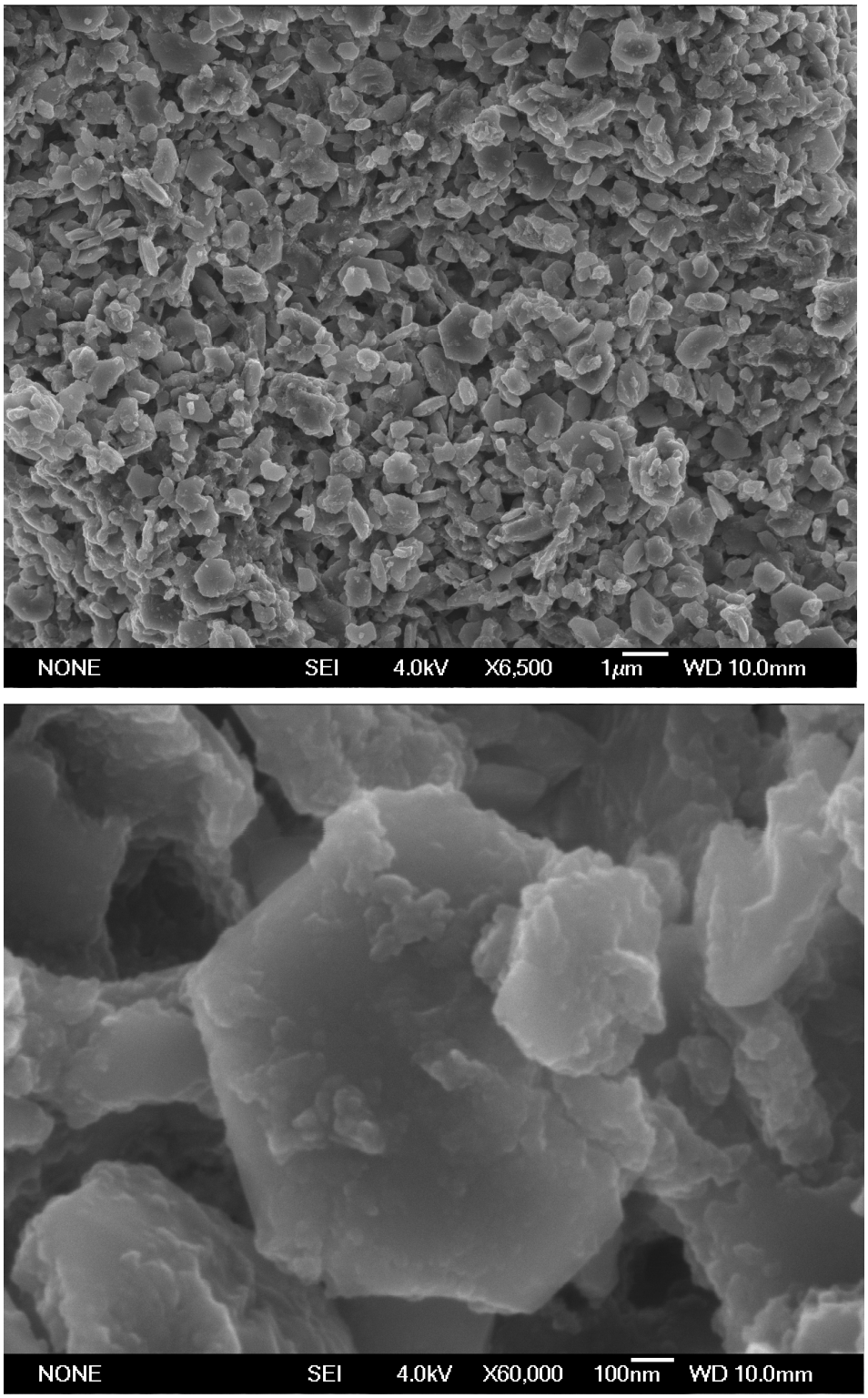

Fig. S5: SEM-micrographs of CAU-6, showing the microcrystalline habitus and the preferentially hexagonal crystal shape.

Thermal Stability. The TG-curve in Fig. S6 shows three steps. During the first weight loss up to ~180 °C, adsorbed solvent is removed from the channels of the MOF, which gives rise to the measured porosity. Two additional steps lead to the decomposition of the framework by further removal of solvent molecules and decomposition of the linker molecules. The measured weight losses (first step: 8 %; second and third step: 58 %, residual mass: 34 %) are in good agreement with the expected value based on the sum formula (expected residual mass: 32.7 %).

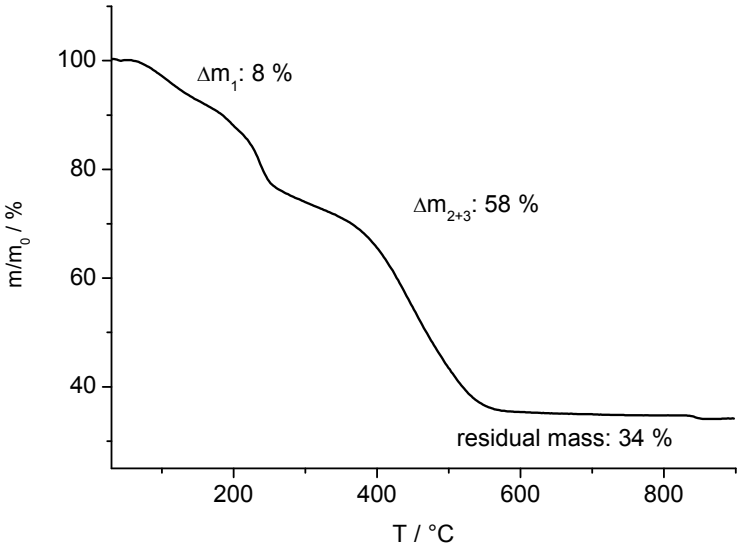

Fig. S6: TG-curve for CAU-6 measured in air with a heating rate of 4 K/min.

The temperature-dependent XRPD-data (Fig. S7) shows an increasing intensity of the peaks up to ~ 240 °C, due to the partial removal of occluded solvent. It further confirms the decomposition above 240 °C. The higher stability compared to TG-data is due to the measurement in a capillary.

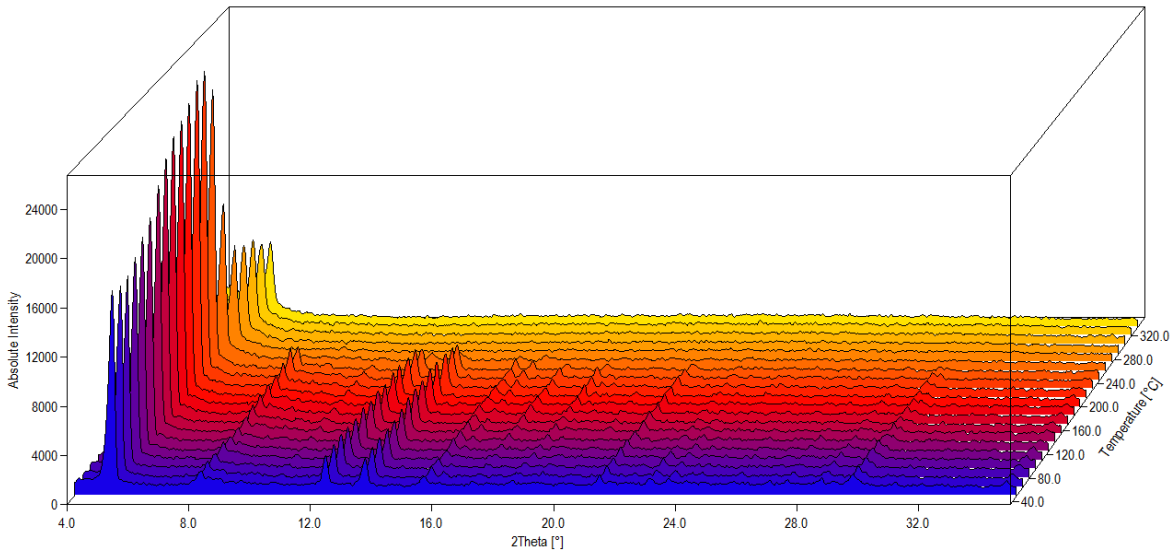

Fig. S7: TDXRD-data for CAU-6 measured in a capillary under air.

Sorption Properties

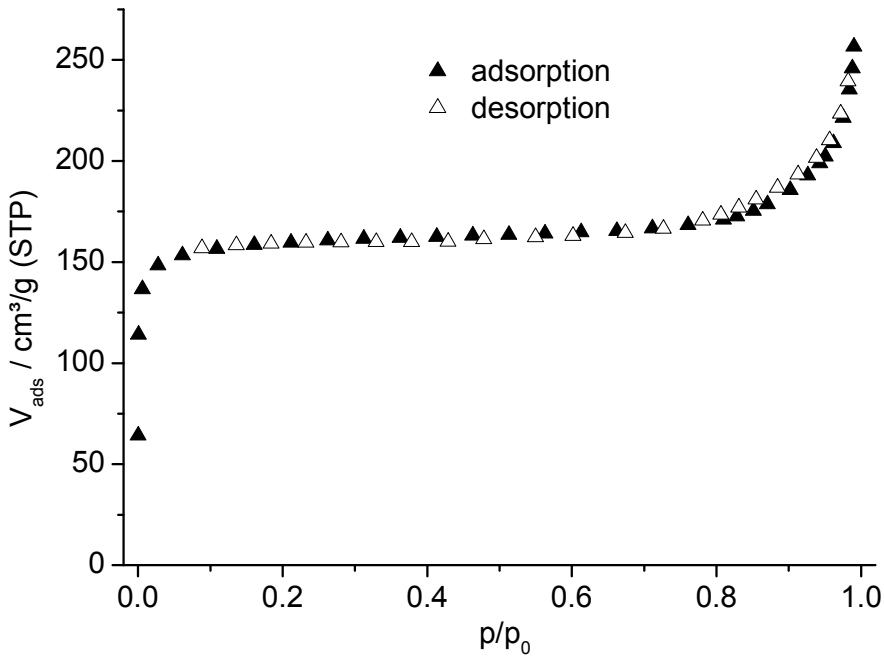

Fig. S8: Nitrogen sorption isotherm measured at 77 K after activation of the MOF at 130 °C in vacuum (0.1 mbar).

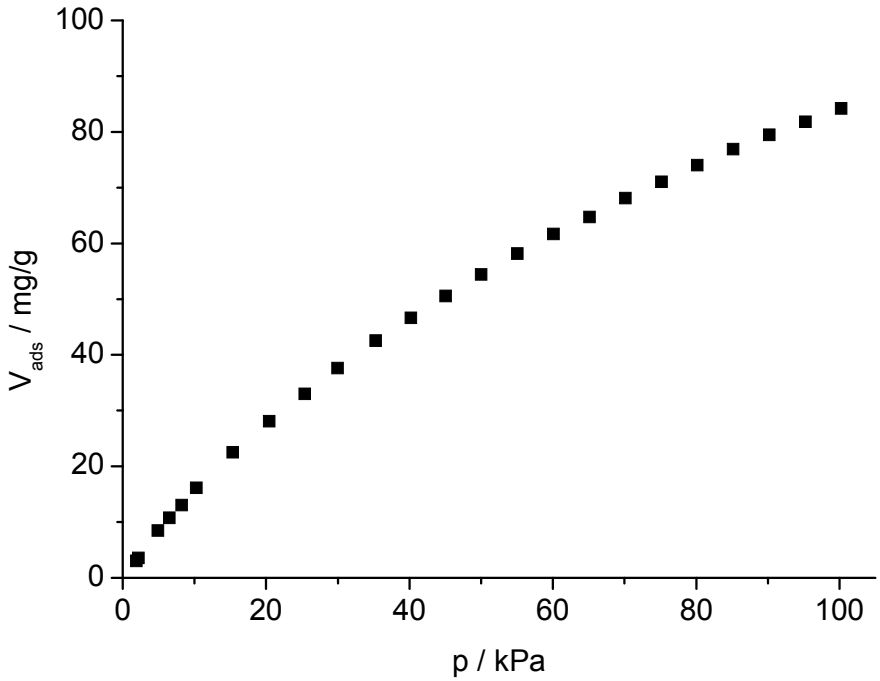

Fig. S9: CO_2 adsorption isotherm measured at 298 K after activation of the MOF at 130 °C in vacuum (0.1 mbar).

S5: XRPD-data and structure determination of CAU-6

Structure Determination. The XRPD-data for structure determination was recorded at the beamline G3 at the DORIS accelerator Ring at the DESY, Hamburg. The MOF was filled into a 0.5 mm capillary and measured with a wavelength of 1.54295 Å. Indexing of the powder pattern resulted in a hexagonal/trigonal cell with the refined cell parameters $a = b =$ 19.2275(3) Å and c = 14.0741(3) Å (Fig. S10). The extinction conditions were suitable for the space groups *P*31*c*, *P*-31*c*, *P*-62*c*, $P6_3mc$ and $P6_3/mmc$.

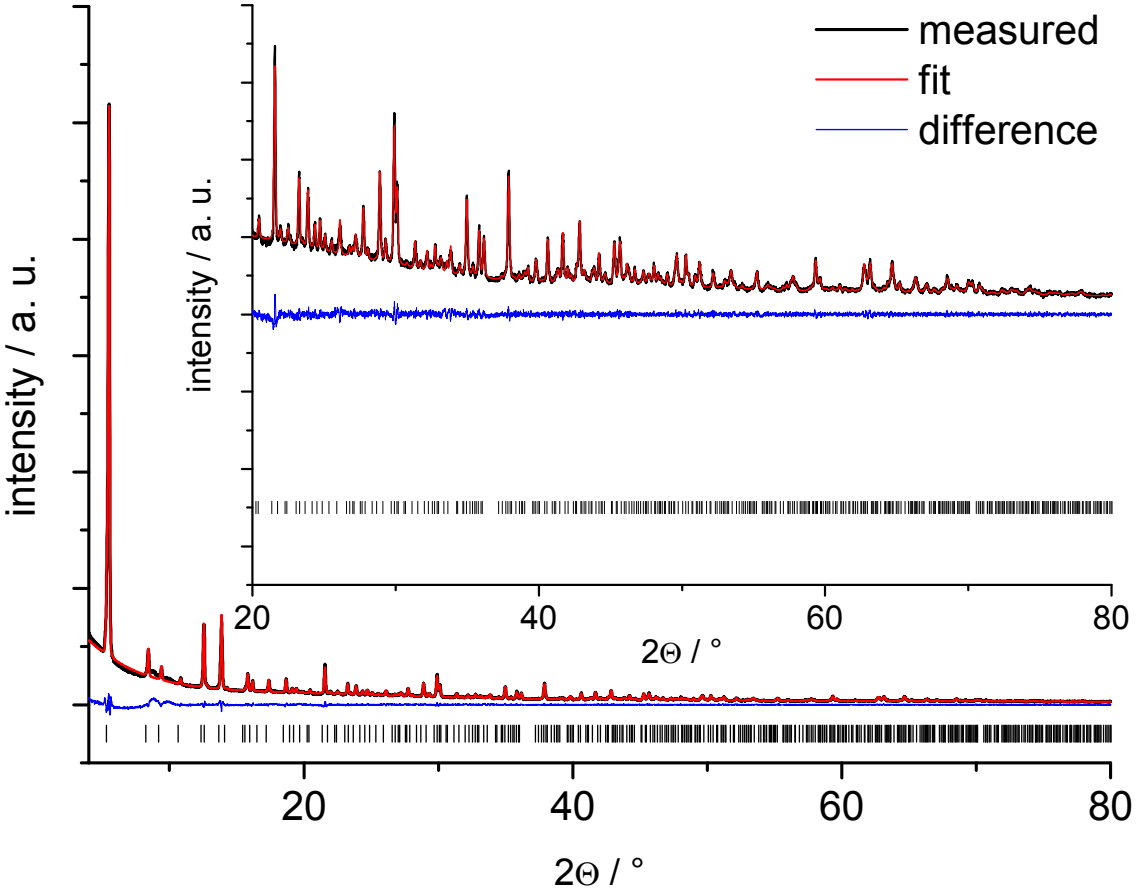

Fig. S10: Le-Bail-fit of CAU-6 in the space group $P6_3/mmc$. The obtained figures of merit are R_{WP} = 5.2 % and R_{exp} = 2.5 %.

The structure solution by direct methods[4] resulted in plausible structural fragments in the space groups *P*-31*c* and *P*-62*c*. The inorganic building units could be unambiguously identified. The structures obtained in *P*-31*c* and *P*-62*c* were found to exhibit the higher symmetry of the space group $P6_3/mmc$, as tested with Material Studio[5] and Platon.[6] Residual electron density indicated, that the carboxylate groups were coordinated to the bridging AlO_6-dimers between the heptanuclear cores. Therefore, the linker molecules were inserted at the corresponding positions and were structurally optimized using force-field methods,

employing Material Studio. We tried to complete this crystallographic model by Fourier-synthesis using TOPAS[7], but none of the remaining fragments (chloride ions, solvent molecules) could be located, even if structural models of lower symmetry were employed. We interpret this as a sign of disorder of the remaining structural fragments. Therefore, the attempted Rietveld refinement did not result in satisfying figures of merit. The measured pattern and a simulated one of the framework model are compared in Fig. S11.

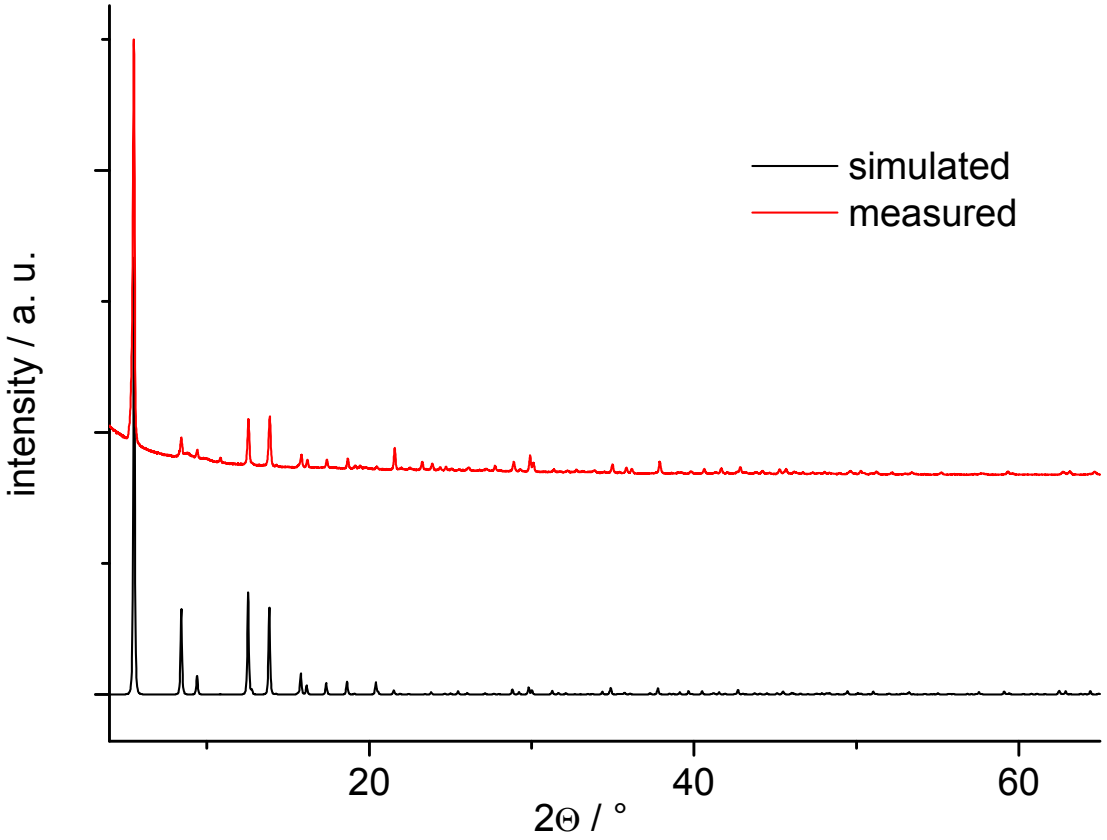

Fig. S11: Comparison of the simulated and the measured XRPD-pattern (λ = 1.54295 Å).

The structural model is given in .cif-format at the end of this document. The asymmetric unit is shown in Fig. S12 and the relevant bond distances are summarized in Tab. S1.

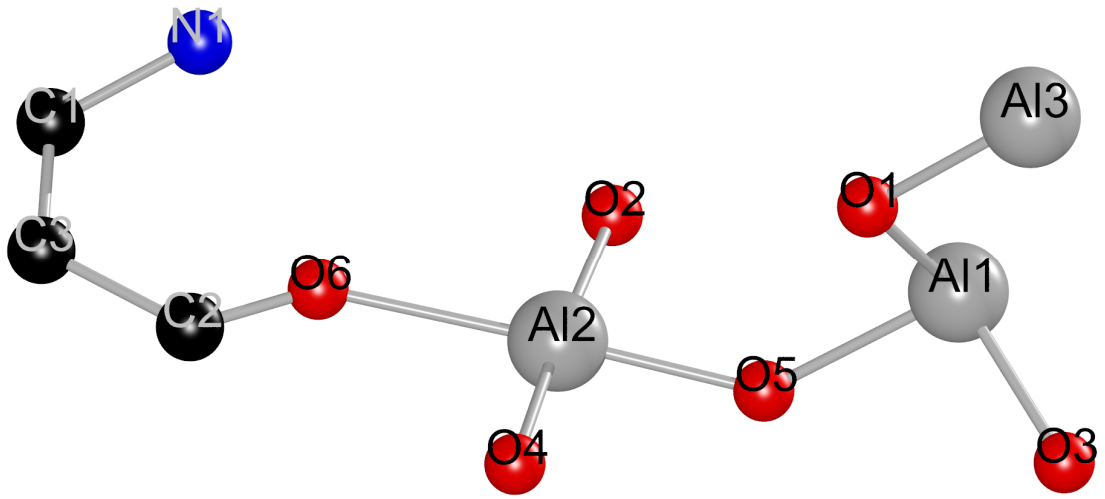

Fig. S12: Asymmetric unit of CAU-6 with numbering scheme as in Tab. S2.

Tab. S2: Bond distances in CAU-6.

Al1	O3	1.8691	Al3	O1	1.7750
	O5	1.8909	O6	C2	1.1544
	O1	2.0229	C1	C1	1.3971
Al2	O5	1.7646		C3	1.4114
	O2	1.9336		N1	1.4281
	O4	1.9985	C2	C3	1.4803
	O6	2.0397	N1	C1	1.4281

Construction principle of the structure of CAU-6 starting from Al_{13}-clusters

The Al_{13} cluster as observed in $[Al_{13}(OH)_{24}(H_2O)_{24}]Cl_{15}\cdot 13H_2O$[8] can be used to construct the framework of CAU-6. Taking into account that bridging between the Al^{3+} ions is exclusively accomplished by OH^- ions (presented as red spheres), condensation of the $[Al_{13}(OH)_{24}(H_2O)_{24}]^{15+}$ ions lead to columns of the composition $[Al_{13}(OH)_{27}(H_2O)_{18}]^{12+}$ (Fig. S13). Water molecules are presented as blue spheres. Twelve water molecules per formula unit are formally replaced by bridging dicarboxylate ions which leads to the final composition $[Al_{13}(OH)_{27}(H_2O)_6(O_2CR)_6]^{6+}$. Since the dicarboxylate ions BDC-NH_2^{2-} are interconnecting the inorganic columns the final framework composition $[Al_{13}(OH)_{27}(H_2O)_6(BDC\text{-}NH_2)_3]^{6+}$ is expected (Fig. S14). This is in agreement with the observed formula.

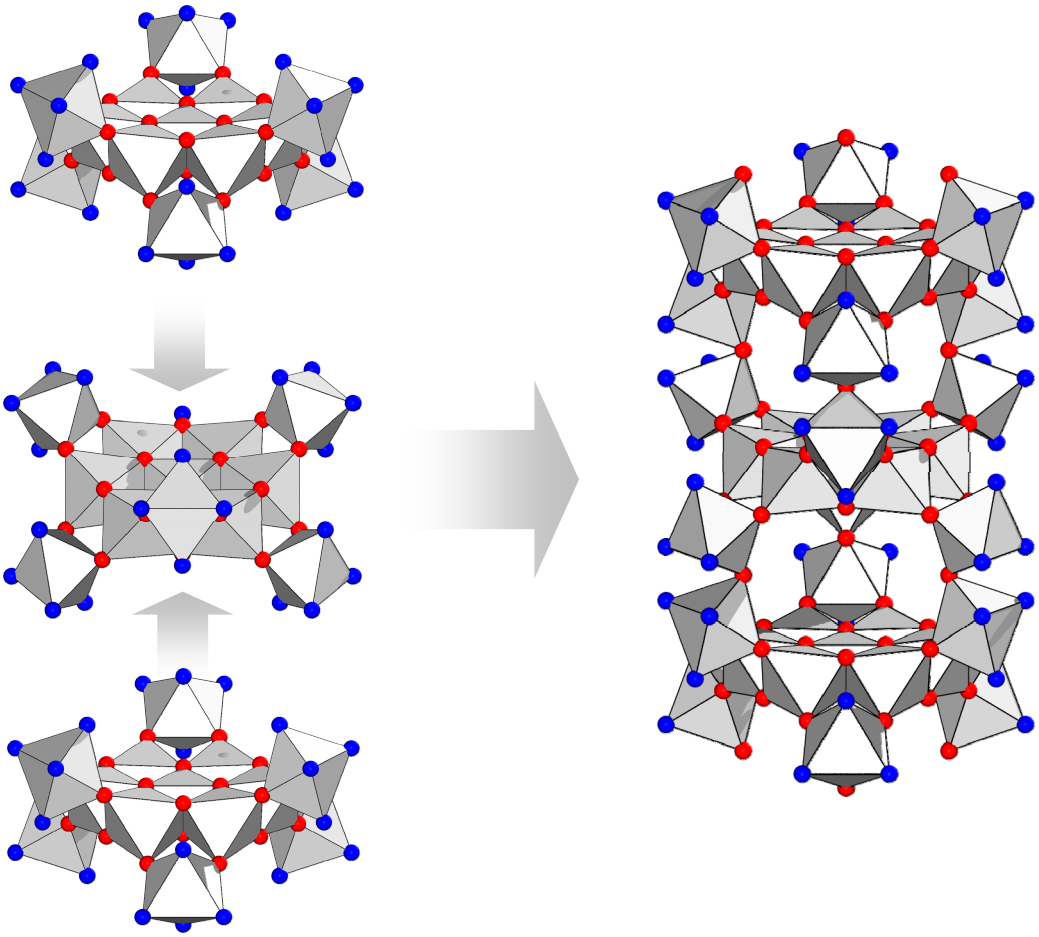

Fig. S13: Schematic representation of the formal condensation of Al_{13}-cluster into the column observed in CAU-6.

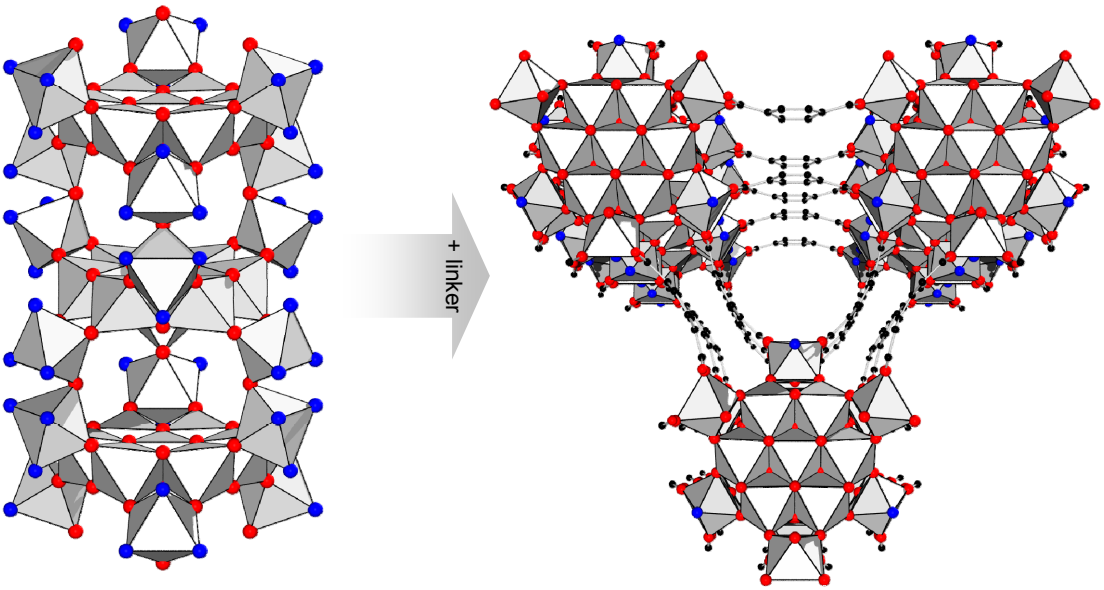

Fig. S14: Schematic representation of the interconnection of columns by linker molecules.

S6: Solid-State NMR-spectra of CAU-6

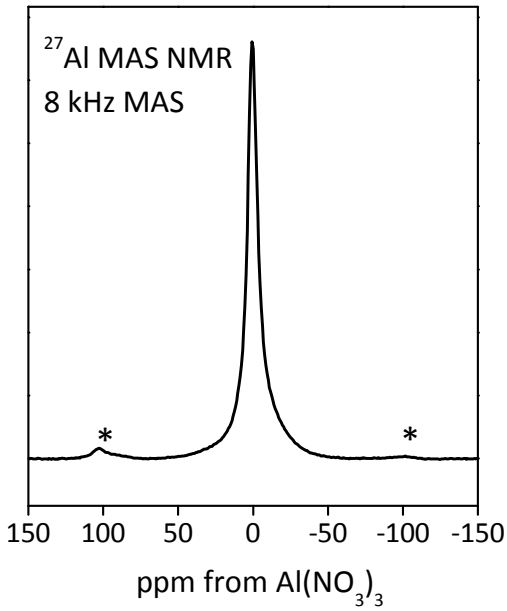

Fig. S15: Solid-state ^{27}Al-MAS-NMR spectrum of CAU-6. The spinning side-bands are marked with asterisks.

The one dimensional ^{27}Al-MAS-NMR spectrum shows that all Al atoms are located in octahedral environment of oxygen atoms in the first coordination sphere. The symmetry of the second coordination sphere is not influencing the symmetry of the AlO_6 units.

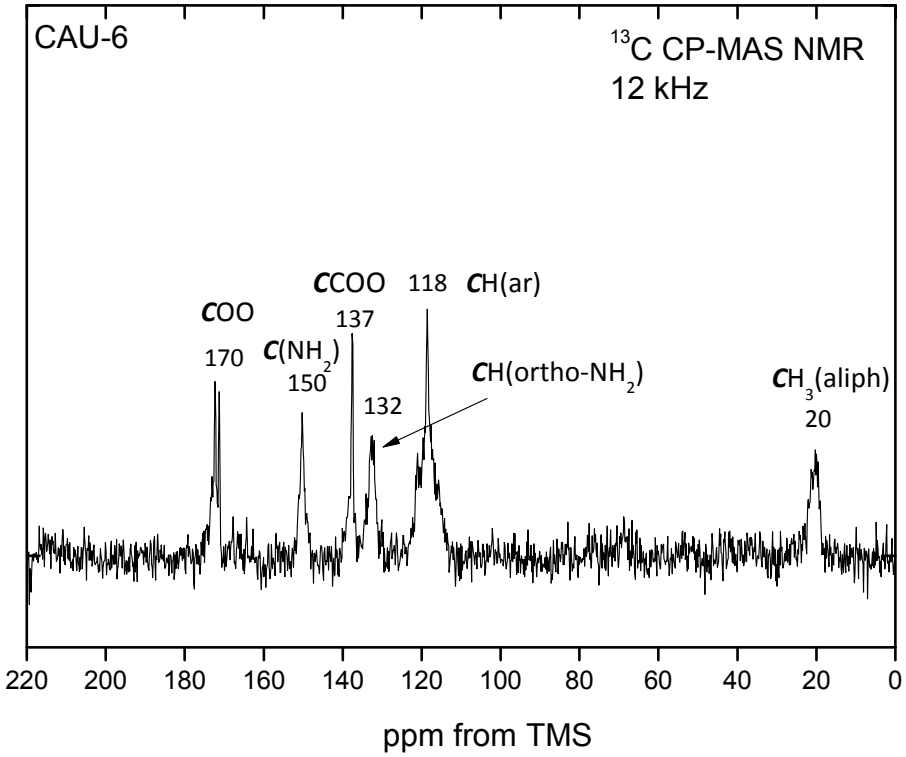

Fig. S16: Solid-state ^{13}C-^{1}H-CP-MAS-NMR spectrum of CAU-6.

The ^{13}C-^{1}H-CP-MAS-NMR spectrum was recorded to characterise the aminoterephthalate ions incorporated in CAU-6. The signals can are assigned in table S3.

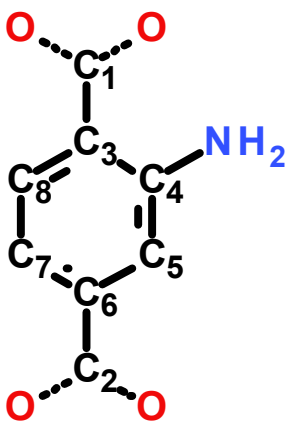

C-atom	Chemical shift (ppm)
C1, C2	170
C4	150
C3, C6	137
C5	132
C7, C8	118

The signal at 20 ppm can be assigned to a CH_3 group from aliphatic species and is due to isopropanol molecules that were not removed by extensive washing.

1D ^{27}Al spectra are broadened due to the strong quadrupolar coupling, hence it is not possible to distinguish between different signals with similar chemical shift. 2D ^{27}Al MQMAS spectrum helps to overcome this problem because it provides the opportunity to separate the CSA interaction from the quadrupolar interaction. The spectrum reveals two different signals caused by different surroundings of aluminium atoms in the structure.

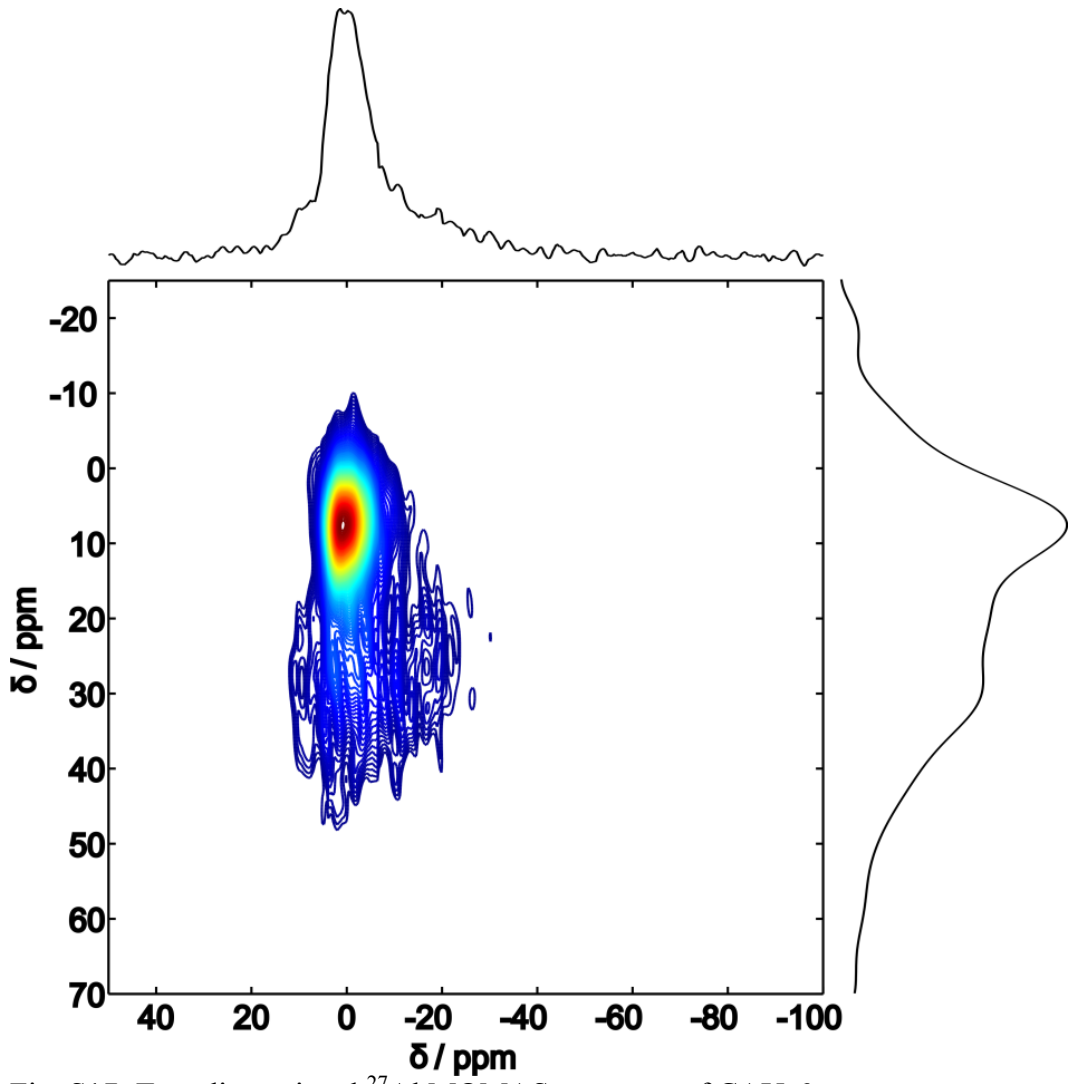

Fig. S17: Two dimensional ^{27}Al MQMAS spectrum of CAU-6.

S7: Temperature-dependent IR-spectra

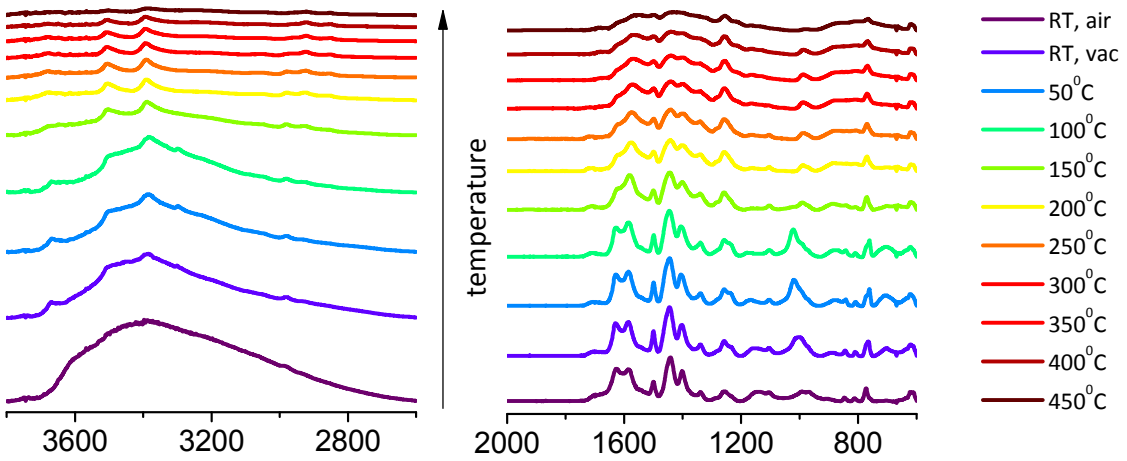

Fig. S18: Temperature-dependent IR spectra of CAU-6. All spectra (except for marked as RT) at 50^{0}C.

The IR spectra show that it is not possible to remove all solvent and/or water molecules from the pores without damaging the framework by thermal activation. The intensity of the broad absorption around 3400 cm^{-1}, characteristic of hydrogen-bonded OH groups, is substantially decreased by applying vacuum and further lowered by heating of the sample (in vacuum). This band can be assigned both to hydrogen-bonded water and propanol. During heating, the OH-band of hydroxyl-groups at 3670 cm^{-1} and the NH_2-bands at 3500 cm^{-1} and 3380 cm^{-1} gain intensity, but already at 150 °C, the peaks in the spectrum are flattened. Decrease of the intensities occurs especially in the region 1800 – 1300 cm^{-1} where C-C- and C=O vibrations are observed and marks the beginning decomposition of the framework. The complete removal of the solvent and water molecules, which is achieved at ~250 °C based on the IR-spectra, the TG-experiments and the TDXRPD-data, thus substantially damages the framework structure. It can be observed that water molecules are removed at lower temperature region: decrease of the intensity of the band at 3400 cm^{-1} is accompanied by the increase of the C-O band at 1025 cm^{-1}.[9] This means that water-propanol interactions are replaced by propanol-propanol interactions and finally, with further temperature increase, by propanol desorption (disappearance of the 1025 cm^{-1} band).

S8: Crystallographic Information File

```
data_CAU-6
_symmetry_space_group_name_H-M    'P63/MMC'
_symmetry_Int_Tables_number       194
_symmetry_cell_setting            hexagonal
loop_
_symmetry_equiv_pos_as_xyz
  x,y,z
  -y,x-y,z
  -x+y,-x,z
  -x,-y,z+1/2
  y,-x+y,z+1/2
  x-y,x,z+1/2
  y,x,-z
  x-y,-y,-z
  -x,-x+y,-z
  -y,-x,-z+1/2
  -x+y,y,-z+1/2
  x,x-y,-z+1/2
  -x,-y,-z
  y,-x+y,-z
  x-y,x,-z
  x,y,-z+1/2
  -y,x-y,-z+1/2
  -x+y,-x,-z+1/2
  -y,-x,z
  -x+y,y,z
  x,x-y,z
  y,x,z+1/2
  x-y,-y,z+1/2
  -x,-x+y,z+1/2
_cell_length_a                19.2275
_cell_length_b                19.2275
_cell_length_c                14.0741
_cell_angle_alpha             90.0000
_cell_angle_beta              90.0000
_cell_angle_gamma            120.0000
loop_
_atom_site_label
_atom_site_type_symbol
_atom_site_fract_x
_atom_site_fract_y
_atom_site_fract_z
_atom_site_U_iso_or_equiv
_atom_site_adp_type
_atom_site_occupancy
Al1    Al    0.15864   0.15864   0.00000   0.02533  Uiso   1.00
Al2    Al    0.30662   0.15331   0.12799   0.02533  Uiso   1.00
Al3    Al    0.00000   0.00000   0.00000   0.02533  Uiso   1.00
O1     O     0.09506   0.04753   0.05707   0.02533  Uiso   1.00
O2     O     0.35854   0.17927   0.00510   0.02533  Uiso   1.00
```

O3	O	0.09789	0.19578	0.06295	0.02533	Uiso	1.00
O4	O	0.24522	0.12261	0.25000	0.02533	Uiso	1.00
O5	O	0.24672	0.19169	0.08346	0.02533	Uiso	1.00
O6	O	0.37641	0.11062	0.18232	0.02533	Uiso	1.00
C1	C	0.49691	0.06648	0.16360	0.02533	Uiso	1.00
C2	C	0.40052	0.09594	0.25000	0.02533	Uiso	1.00
C3	C	0.46280	0.07214	0.25000	0.02533	Uiso	1.00
N1	N	0.46119	0.06657	0.07467	0.02533	Uiso	0.25

Literature

1 J.P. Amoreux, C. Fernandes, S. Steuernagel, *J. Magn. Reson. A*, 1996, **123**, 116.
2 A. Jerschow, R.J. Kumar, *J. Magn. Reson*, 2003, **160**, 59.
3 K. Barthelet, J. Marrot, G. Férey, D. Riou, *Chem. Commun.* 2004, 520.
4 A. Altomare, M. Cavalli, R. Calandro, C. Cuocci, C. Giacovazzo, A. Gagliardi, A. G. G. Moliterni, R. Rizzi, EXPO2004. Program for Solving Crystal Structures from Powder Data by direct Methods, 2004.
5 Materials Studio Version 5.0, Accelrys Inc., San Diego, CA, 2009.
6 A.L. Spek, PLATON, A Multipurpose Crystallographic Tool, Utrecht University, Utrecht, The Netherlands, 2010.
7 Topas Academics 4.2, Coelho Software, 2007.
8 W. Seichter, H. Mögel, P. Brand, D. Salah, *Eur. J. Inorg. Chem.* 1998, **6**, 795.
9 J.J. Max, C. Chapados, *J. Chem. Phys.,* 2009, **130**, 124513.